The Astrophysical Journal, 934:93 (9pp), 2022 August 1 https://doi.org/10.3847/1538-4357/ac7a45
© 2022. The Author(s). Published by the American Astronomical Society.
OPEN ACCESS

Slowly Cooling White Dwarfs in NGC 6752

Jianxing Chen[1,2], Francesco R. Ferraro[1,2], Mario Cadelano[1,2], Maurizio Salaris[3,4], Barbara Lanzoni[1,2], Cristina Pallanca[1,2], Leandro G. Althaus[5,6], Santi Cassisi[4,7], and Emanuele Dalessandro[2]
[1] Dipartimento di Fisica e Astronomia "Augusto Righi", Alma Mater Studiorum Università di Bologna, via Piero Gobetti 93/2, I-40129 Bologna, Italy
francesco.ferraro3@unibo.it
[2] INAF-Osservatorio di Astrofisica e Scienza dello Spazio di Bologna, Via Piero Gobetti 93/3, I-40129 Bologna, Italy
[3] Astrophysics Research Institute, Liverpool John Moores University, Liverpool Science Park, IC2 Building, 146 Brownlow Hill, Liverpool L3 5RF, UK
[4] INAF-Osservatorio Astronomico d'Abruzzo, Via Maggini, I-64100 Teramo, Italy
[5] Grupo de Evolucion Estelar y Pulsaciones, Facultad de Ciencias Astronómicas y Geofisicas, Universidad Nacional de La Plata, Paseo del Bosque s/n, 1900 La Plata, Argentina
[6] Centro Científico Tecnológico CONICET La Plata, Consejo Nacional de Investigaciones Científicas y Técnicas, Calle 8 No. 1467, B1904CMC La Plata, Buenos Aires, Argentina
[7] INFN—Sezione di Pisa, Largo Pontecorvo 3, I-56127 Pisa, Italy
Received 2022 May 2; revised 2022 June 14; accepted 2022 June 16; published 2022 July 28

Abstract

Recently, a new class of white dwarfs ("slowly cooling WDs") has been identified in the globular cluster M13. The cooling time of these stars is increased by stable thermonuclear hydrogen burning in their residual envelope. These WDs are thought to be originated by horizontal branch (HB) stars populating the HB blue tail that skipped the asymptotic giant branch phase. To further explore this phenomenon, we took advantage of deep photometric data acquired with the Hubble Space Telescope in the near-ultraviolet and investigate the bright portion of the WD cooling sequence in NGC 6752, another Galactic globular cluster with a metallicity, age, and HB morphology similar to M13. The normalized WD luminosity function derived in NGC 6752 turns out to be impressively similar to that observed in M13, in agreement with the fact that the stellar mass distribution along the HB of these two systems is almost identical. As in the case of M13, the comparison with theoretical predictions is consistent with ∼70% of the investigated WDs evolving at slower rates than standard, purely cooling WDs. Thanks to its relatively short distance from Earth, NGC 6752 photometry reaches a luminosity 1 order of a magnitude fainter than the case of M13, allowing us to sample a regime where the cooling time delay, with respect to standard WD models, reaches ∼300 Myr. The results presented in this paper provide new evidence for the existence of slowly cooling WDs and further support to the scenario proposing a direct causal connection between this phenomenon and the HB morphology of the host stellar cluster.

Unified Astronomy Thesaurus concepts: Globular star clusters (656); Hertzsprung Russell diagram (725); White dwarf stars (1799); Ultraviolet photometry (1740)

1. Introduction

White dwarfs (WDs) are the final evolutionary stage of the vast majority (∼98%) of stars in the universe (Winget & Kepler 2008). Indeed, all stars with an initial mass below 8 $M_{\odot}$, with a possible extension to 11 $M_{\odot}$, are expected to end their evolution as WDs (Woosley & Heger 2015; Córsico et al. 2019). Their study can provide a large amount of information about the physical properties and the evolutionary mechanisms of their progenitors. Moreover, WDs are the ideal stellar structures to test physical processes occurring under extreme matter density conditions.

WDs are commonly envisaged as the naked cores of the progenitor stars that, at the end of their life, have lost the envelope. Their evolution in time is generally described as a pure cooling process, during which WDs evolve toward cooler temperatures and fainter luminosities because essentially they cannot produce energy, either through nuclear reactions, or by gravitational contraction, and radiate away the residual thermal energy of their ions. This produces a tight relation between WD luminosities and their cooling ages, which has been commonly adopted as a cosmic chronometer to constrain the age of several populations of our Galaxy, including the disk, globular, and open clusters (e.g., Hansen et al. 2007; Bedin et al. 2010; Jeffery et al. 2016; Kilic et al. 2017).

However, recent models (Althaus et al. 2015) show that even an extraordinary small amount of residual hydrogen (a few $10^{-4}\,M_{\odot}$) left over from the previous evolutionary stages is sufficient to allow quiescent thermonuclear burning. This can provide a nonnegligible source of energy that slows down the cooling rate, especially in the low-mass ($<0.6\,M_{\odot}$) and low-metallicity ($Z < 0.001$) regimes, which are typical of globular clusters (GCs) in the Galactic halo. In turn, an increased evolutionary timescale naturally translates to an increased number of WDs for any fixed luminosity, with a consequent observable impact on the WD luminosity function (LF).

The first observational evidence of slowly cooling WDs has been recently provided (Chen et al. 2021, hereafter C21) by the analysis of Hubble Space Telescope (HST) ultradeep photometric data acquired in the near-ultraviolet (near-UV) for M3 (NGC 5272) and M13 (NGC 6205). These two Galactic GCs are considered "twin" systems because they have very similar iron abundance ($[Fe/H] \simeq -1.5$), age ($t \sim 12.5$ Gyr), total mass, and central density (see, e.g., C21). In spite of such a similarity, C21 discovered a clear excess of WDs in the LF of M13 with respect to M3, and showed that the detected

Original content from this work may be used under the terms of the Creative Commons Attribution 4.0 licence. Any further distribution of this work must maintain attribution to the author(s) and the title of the work, journal citation and DOI.

Table 1
Main Physical Parameters of NGC 6752

Parameter		References
$E(B-V)$	0.046 ± 0.005	Gratton et al. (2005)
	0.040	Harris (1996) (2010 edition)
$[Fe/H]$	-1.48 ± 0.01	Gratton et al. (2005)
	-1.54	Harris (1996) (2010 edition)
$(m-M)_0$	13.13	Ferraro et al. (1999)
Age (Gyr)	12.5 ± 0.75	Dotter et al. (2010)
$\log \nu_0$ ($L_\odot/pc^3$)	5.04	Harris (1996) (2010 edition)
$\log t_{rc}$ (yr)	6.88	Harris (1996) (2010 edition)

overabundance is very well described by assuming that ∼70% of the WD population in M13 is composed of slowly cooling objects, while the objects in M3 cool down as expected from standard models. This result is fully consistent also with the different morphology of the horizontal branch (HB) observed in the two systems (e.g., Ferraro et al. 1997a; Dalessandro et al. 2013): The HB of M13 shows a pronounced extension to the blue, while no blue tail is observed in M3, where the HB is populated in both the red and the blue side of the instability strip, with a sizeable population of RR Lyrae stars. The different morphology is the direct manifestation of different stellar mass distributions along the HB, with the stars populating the blue tail of M13 being less massive than those at the red edge, and those on the M3 HB. In turn, the stellar mass during the HB phase is the parameter mainly determining the occurrence (or not) of the so-called "third dredge-up," a mixing process taking place during the asymptotic giant branch (AGB) phase, which is the evolutionary phase immediately following the HB and preceding the WD stage. This process efficiently mixes the material present in the envelope of AGB stars, bringing most of the hydrogen deeper into the stellar interior, where it is burned. As a consequence, stars experiencing the third dredge-up reach the WD stage with not enough residual hydrogen to have an efficient burning. On the other hand, stars evolving from the blue side of the HB have envelope masses too small to reach the AGB and therefore do not experience the third dredge-up, and they reach the WD stage with a residual hydrogen envelope thick enough to sustain stable thermonuclear burning, thus delaying their aging (Althaus et al. 2015). Most of the stars in M13 (those populating the blue side of the HB) skip the third dredge-up (the so-called post-early AGB and AGB-manqué stars) ending their lives as slowly cooling WDs. On the other hand, according to the observed HB morphology, the HB stars in M3 have large enough masses to reach the AGB and therefore evolve later as standard WDs. The presence of slowly cooling WDs in M13 and the lack thereof in M3 explains the observed numerical excess in the LF of the former.

C21 therefore demonstrated that the presence of slowly cooling WDs can be recognized from the analysis of the WD LF, and it is causally connected to the HB morphology. Specifically, slowly cooling WDs are expected in clusters with moderate metallicity and blue-tail HB. In this context, here we present the analysis of the bright portion of the WD cooling sequence of NGC 6752, a Galactic GC with a metal abundance and HB morphology very similar to those of M13 (see its main parameters in Table 1). NGC 6752 and M13 also share a very low value of the R_2 parameter, defined as the ratio between the number of AGB and that of HB stars: $R_2 = N_{AGB}/N_{HB} = 0.06$–$0.07$ (Sandquist & Bolte 2004; Cho et al. 2005; Cassisi et al. 2014). This is consistent with the findings of Gratton et al. (2010), who empirically showed that the R_2 parameter correlates with the HB morphology (clusters with blue extended HB have lower R_2 values), because the stars located in the bluest portion of the HB skip the AGB phase.[8] The simulations of Cassisi et al. (2014) also confirmed that the parameter R_2 of NGC 6752 is well reproduced by standard HB models, and they show that the distribution of stellar masses along the HB in this cluster is essentially the same as in M13 (Dalessandro et al. 2013).

Because of its similarity with M13 in terms of metallicity ([Fe/H] ∼ −1.5; Gratton et al. 2005), age ($t \sim 12.5$ Gyr; e.g., Salaris & Weiss 2002; Dotter et al. 2010; VandenBerg et al. 2013), HB morphology, and HB mass distribution, NGC 6752 thus offers the ideal conditions to further test the presence of a substantial population of slowly cooling WDs in GCs with blue HB morphology. Being closer to Earth than M13, it also allows us to extend the study of this new class of objects to fainter magnitudes.

The paper is organized as follows. Section 2 describes the adopted data reduction, calibration, and completeness correction procedures. The analysis of the WD cooling sequence and LF is presented in Section 3, which is followed by the discussion of the results and conclusions in Section 4.

2. Data Reduction

The high-resolution photometric data set of NGC 6752 used in this work has been acquired in the near-UV with the HST under GO-12311 (PI: Piotto) and GO-11729 (PI: Holtzman), using the UVIS channel of the Wide Field Camera 3 (WFC3). It is composed of 12 long exposures (369 s each) in the F275W filter and 3 images in the F336W (2×500 s, and 1×30 s).

The photometric analysis was carried out on the *_flc* images (which are the UVIS calibrated frames, also corrected for charge transfer efficiency), after applying the Pixel Area Map (PAM) correction. We used DAOPHOT IV (Stetson 1987) to follow the so-called "UV-route," which consists of first searching for stellar sources in the near-UV images, then force-fitting the source detection at the same positions of the UV-selected stars in longer wavelength images (Ferraro et al. 1997b, 2001, 2003; Raso et al. 2017; Dalessandro et al. 2018b, 2018a; Cadelano et al. 2019, 2020a). This procedure allows the optimal recovering of blue and faint objects, like WDs, because the crowding effect generated by giants and main-sequence turnoff (MS-TO) stars (which get brighter with increasing wavelengths) is strongly mitigated in near-UV images of old stellar populations (as Galactic GCs).

At first we selected ∼250 bright and unsaturated stars, relatively uniformly distributed in the sampled field of view, to determine the point-spread function (PSF) function of each exposure. The resulting model was then applied to all the sources detected above 5σ from the background, and the stars found at least in half of the UV images were combined to create a *master list*. The photometric fit was then forced in all the other frames at

[8] Note that Campbell et al. (2013; see also Campbell et al. 2017) claimed that all stars of second generation (i.e., with [Na/Fe] < 0.2; see Gratton et al. 2012 for a review) skip the AGB. However, this result has been challenged by synthetic HB simulations (Cassisi et al. 2014), and by both spectroscopic (Lapenna et al. 2016; Mucciarelli et al. 2019) and photometric observations (Gruyters et al. 2017) that found evidence of both first- and second-generation stars along the AGB of NGC 6752.

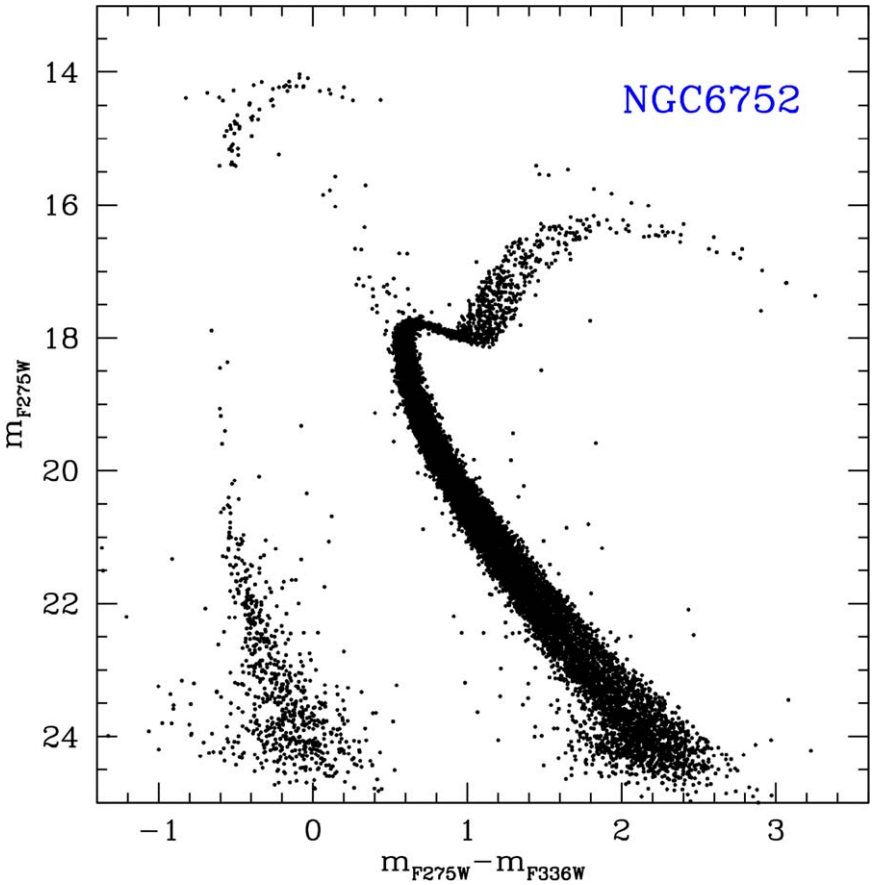

Figure 1. Near-UV color–magnitude diagram (CMD) of NGC 6752.

the positions corresponding to the master list stars, by using DAOPHOT/ALLFRAME (Stetson 1994). Finally, the magnitudes estimated for each star in different images of the same filter were homogenized, and their weighted mean and standard deviation have been adopted as the star's magnitude and its related photometric error. The instrumental magnitudes were calibrated to the VEGAMAG system and the instrumental coordinates, once corrected for geometric distortions, have been put onto the International Celestial Reference System by cross correlation with the catalog obtained from the HST UV Globular Cluster Survey (Piotto et al. 2015). A selection in sharpness was applied to remove nonstellar objects (background galaxies) mainly affecting the faintest end of the sample. All stars with a sharpness parameter larger than 0.2 have been removed. An accurate additional visual inspection of the images was then necessary to decontaminate the sample from spurious detections and artifacts in the regions surrounding heavily saturated stars (Annunziatella et al. 2013).

2.1. Color–Magnitude Diagram and Comparison with M13

The final (m_{F275W}, $m_{F275W} - m_{F336W}$) color–magnitude diagram (CMD) of NGC 6752 is shown in Figure 1. It spans approximately 11 mag, providing us with a full view of the cluster stellar population down to nearly $m_{F275W} = 25$, and with a clear definition of all the evolutionary sequences. As expected in the UV band, the luminosity of red giant branch (RGB) stars is substantially decreased with respect to optical wavelengths, while hot HB stars are the brightest objects. Also a sparse population of blue straggler stars is clearly visible (see Sabbi et al. 2004), covering a magnitude range comparable to that spanned by the RGB. Notably, the bright portion of the WD cooling sequence appears well defined and populated, reaching luminosities comparable to those of MS-TO stars, and covering ∼6 mag in the CMD.

The comparison with Figure 1 of C21 reveals that the overall morphology of the CMD evolutionary sequences in NGC 6752 is very similar to that observed in M13. Indeed, the MS-TO and the subgiant branch can be adopted as optimal reference sequences to determine the shifts in magnitude and color needed to superpose one CMD on the other. We found that a magnitude shift $\Delta m_{F275W} = -1.04 \pm 0.02$ and a small color shift $\Delta(m_{F275W} - m_{F336W}) = +0.04 \pm 0.01$ are required to move the CMD of M13 onto that of NGC 6752. The measured differences are compatible with the shorter distance (∼3 kpc closer; Ferraro et al. 1999) and the larger reddening ($\delta E(B-V) = 0.02-0.03$; see Table 1 and Harris 1996) of NGC 6752 with respect to M13. Indeed the superposition provides an impressive match of all the evolutionary sequences, including the cooling sequence (see Figure 2). In particular we notice that, although being less populated, the HB of NGC 6752 shares the same morphology observed in M13: HB stars are distributed over the same color range, $-0.6 < (m_{F275W} - m_{F336W}) < 0.4$, with no redder HB stars being detected in both clusters. Also the WD cooling sequences are well superposed, with that in NGC 6752 reaching fainter magnitudes, consistently with its shorter distance from Earth.

2.2. Artificial Star Tests

To perform a quantitative study of the WD population of NGC 6752 in terms of star counts, it is necessary to take into

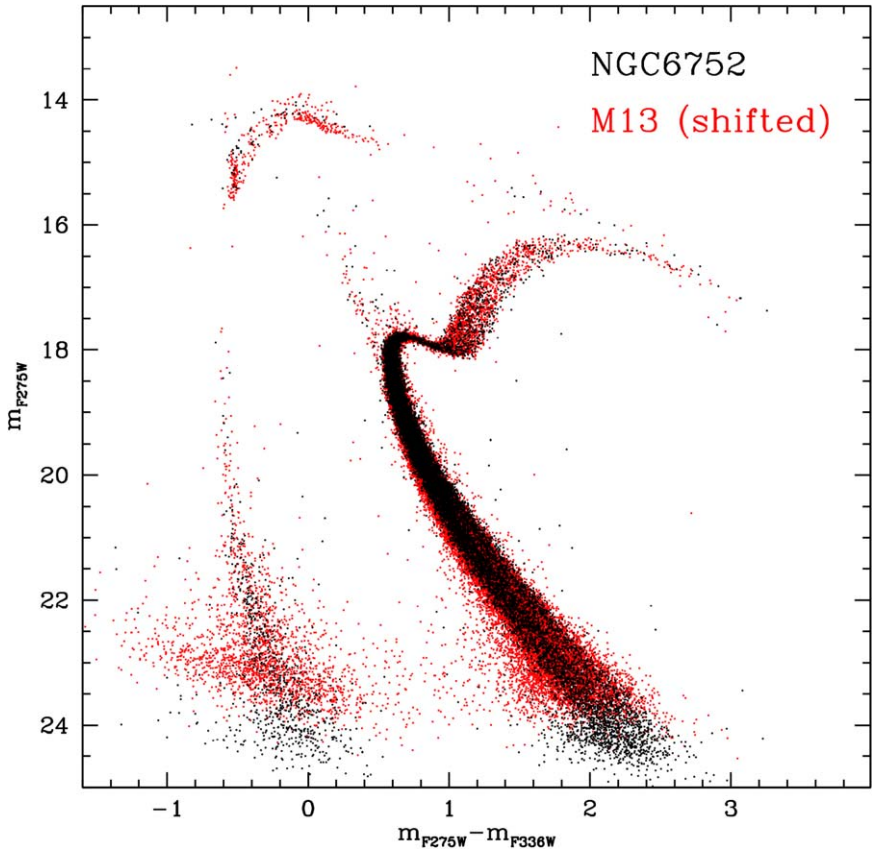

Figure 2. Observed coadded $m_{\rm F275W}$, $m_{\rm F275W} - m_{\rm F336W}$ CMDs of NGC 6752 (black dots) and M13 (red dots, from C21). A magnitude shift $\Delta m_{\rm F275W} = -1.04$ and a color shit $\Delta(m_{\rm F275W} - m_{\rm F336W}) = 0.04$ have been applied to the CMD of M13 to match that of NGC 6752.

account the photometric completeness of the WD cooling sequence at different magnitudes and different distances from the cluster center. This is particularly important in dynamically evolved stellar systems like NGC 6752, which is classified as a post core collapse cluster (Harris 1996). Indeed, the innermost portion ($r < 10''$) of the stellar density profile shows a clear excess with respect to the King (1966) model that properly fits the external regions (Ferraro et al. 2003), consistently with its post core collapse classification.[9]

To estimate the photometric completeness, we performed artificial star experiments following the prescriptions described in detail in Bellazzini et al. (2002; see also Dalessandro et al. 2015; Cadelano et al. 2020b), which we summarize quickly here. As first step, we created a list of artificial stars with an input F275W magnitude sampling the observed extension of the WD cooling sequence. Then, each of these stars was assigned a F336W magnitude obtained by interpolating along the mean ridge line of the WD cooling sequence in the ($m_{\rm F275W}$, $m_{\rm F275W} - m_{\rm F336W}$) CMD. The artificial stars thus generated were then added to the real images by using the DAOPHOT/ADDSTAR software, and the entire photometric analysis was repeated following exactly the same steps described in Section 2. To avoid artificial crowding, the added stars were placed into the frames in a regular grid of 23×23 pixels (corresponding to about 15 times the FWHM of stellar sources), each cell containing only one artificial star during each run. The procedure was iterated several times and, at the end, more than 100,000 artificial stars were simulated in the entire field of view.

The ratio between the number of artificial stars recovered at the end of the photometric analysis (number of output stars, N_o) and the number of stars that were actually simulated (number of input stars, N_i) defines the completeness parameter $\Phi = N_o/N_i$. As is well known, the value of Φ strongly depends on both crowding (hence, the distance from the cluster center) and stellar luminosity, becoming increasingly smaller in cluster regions of larger density and at fainter magnitudes. We thus split the sample of simulated stars into bins of cluster-centric distances (stepped by $5''$) and F275W magnitudes (from $\sim$18 to $\sim$25, in steps of 0.5 mag) and, for each cell of this grid, we counted the number of input and recovered stars, calculating the corresponding value of Φ. The sizes of the radial and magnitude bins were chosen to secure enough statistics while keeping as high as possible both the spatial resolution, and the sensitivity of the completeness curve to changes in the stellar luminosity. The uncertainties assigned to each completeness value (σ_Φ) were then computed by propagating the Poissonian errors, and typically are on the order of 0.05. As coordinates of the center of gravity we adopted the values quoted in Ferraro et al. (2003): $C_{\rm grav}$ is located at $\alpha_{\rm J2000} = 19^{\rm h}10^{\rm m}52\overset{\rm s}{.}04$, $\delta_{J2000} = -59°59'04\overset{''}{.}64$ with a typical 1σ uncertainty of $0\overset{''}{.}5$ in both $\alpha_{\rm J2000}$ and δ_{J2000}. The $C_{\rm grav}$ has been computed by averaging the coordinates of all stars detected in the central portion of the cluster (see Lanzoni et al. 2007, 2010, 2019; Miocchi et al. 2013).

The construction of such a completeness grid allowed us to assign the appropriate Φ value to each observed WD, with a

[9] The advanced stage of dynamical evolution of this system is further certified by the high radial concentration of its blue straggler stars (see Lanzoni et al. 2016; Ferraro et al. 2018), which is a powerful indicator of dynamical age (the "dynamical clock"; see Ferraro et al. 2012, 2018, 2019, 2020).

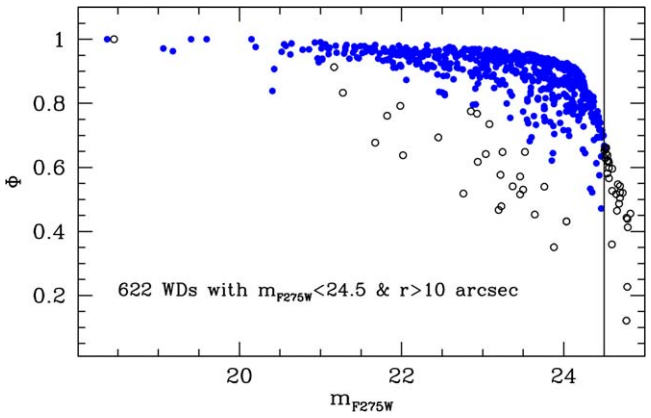

Figure 3. Distribution of the WD completeness parameter Φ, as a function of the F275W magnitude. The 622 selected WDs are plotted as blue circles: they all have $\Phi > 0.45$, while those fainter than $m_{F275W} = 24.5$, or located at distances smaller than 10″ from the cluster center (empty circles) have been excluded from the analysis, to avoid the risk of inappropriate completeness corrections.

given F275W and F336W magnitude, located at any distance from the cluster center. The behavior of the completeness parameter as a function of magnitude is shown in Figure 3 for all the detected WDs. By excluding the overcrowded innermost region ($r < 10''$) and the faintest end ($m_{F275W} > 24.5$) of the cooling sequence (empty circles in the figure), we obtain a well-sampled population of 622 WDs with a completeness level larger than 45% (blue circles).

3. Analysis and Results

3.1. Sample Selection and WD LF

The impressive match between the CMDs of NGC 6752 and M13 shown in Figure 2 allows us to perform a direct comparison among the properties of the two clusters, even using the same set of isochrones and cooling tracks adopted in C21 for M13. Indeed, Figure 4 shows the cooling track of a 0.54 $M_\odot$ carbon–oxygen core WD with a hydrogen atmosphere (DA-type) from Salaris et al. (2010) nicely reproducing the position of the observed WD cooling sequence, and the 12.5 Gyr α-enhanced isochrone with metal abundance $Z = 0.001$ and helium mass fraction $Y = 0.246$ from the BaSTI models (Pietrinferni et al. 2006; see also Hidalgo et al. 2018; Pietrinferni et al. 2021) simultaneously reproducing the MS-TO region of the cluster.

The well-defined cooling sequence in the CMD allowed us to select the WD sample straightforwardly. First, we excluded the objects located more than 3σ away from the mean ridge line of the WD cooling sequence, with σ being the photometric error at the corresponding magnitude level. Then, as discussed above, we conservatively selected stars located at distances larger than 10″ from the cluster center and at magnitudes $m_{F275W} \leqslant 24.5$, to keep the completeness level above 45%. The adopted magnitude cut corresponds to a cooling time of ∼460 Myr, significantly longer than the case of M13, where the analysis was limited to the first 100 Myr of cooling (see C21). Thus, the cooling time sampled by the WD sequence in NGC 6752 is of the order of 0.5 Gyr. Although this is a significant range of cooling times, it corresponds to a negligible variation in terms of WD mass: indeed, the expected difference in mass between a WD that is currently starting the cooling process, and a WD with a cooling age of 0.5 Gyr is 0.001 $M_\odot$ only.

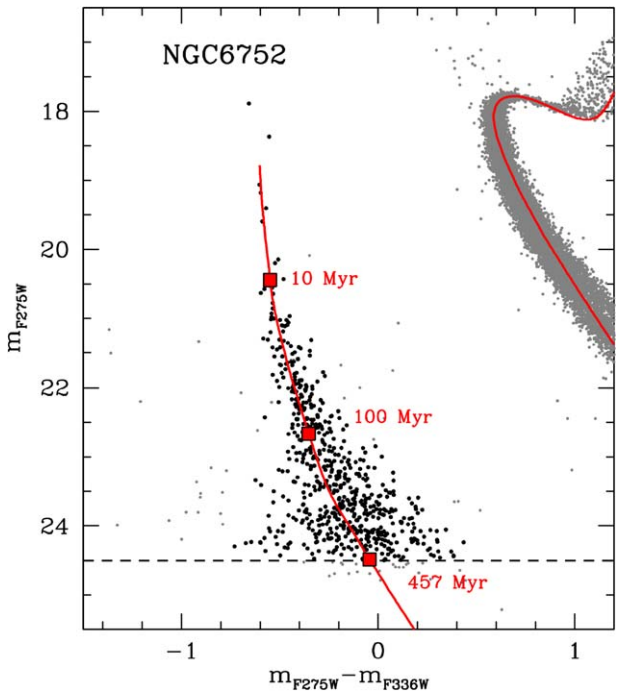

Figure 4. CMD on NGC 6752 zoomed on the WD cooling sequence, with the WD samples selected for analysis denoted by black dots. The red lines are the same set of theoretical models used in C21 to reproduce the evolutionary sequences observed in M13: a 12.5 Gyr old isochrone from the BaSTI data set (Pietrinferni et al. 2006) well fitting the cluster MS, and the cooling sequence of a 0.54 $M_\odot$ hydrogen atmosphere carbon–oxygen WD from Salaris et al. (2010). The red squares flag three cooling ages along the cooling track. The dashed horizontal line marks the adopted magnitude limit of the analyzed WD sample, corresponding to a cooling age $t_{cool} < 460$ Myr.

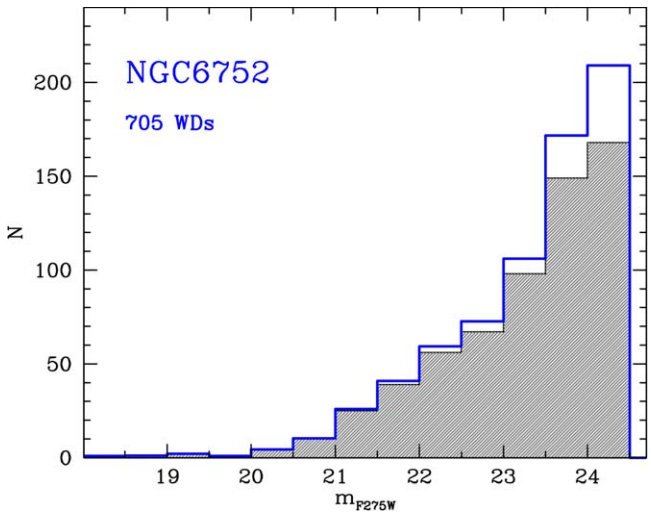

Figure 5. Observed and completeness corrected luminosity functions (shaded and blue histograms, respectively) obtained from the selected WD sample (black dots in Figure 4).

The adopted selection criteria provide a total of 622 WDs in NGC 6752. The LFs computed in bins of 0.5 mag are shown in Figure 5 for both the observed and the completeness corrected samples (shaded and blue histograms, respectively). It can be seen that the conservative criteria adopted for the sample selection strongly limit the impact of incompleteness: the global correction to the adopted samples is smaller than 15%, with the completeness corrected population of WDs counting 705 stars.

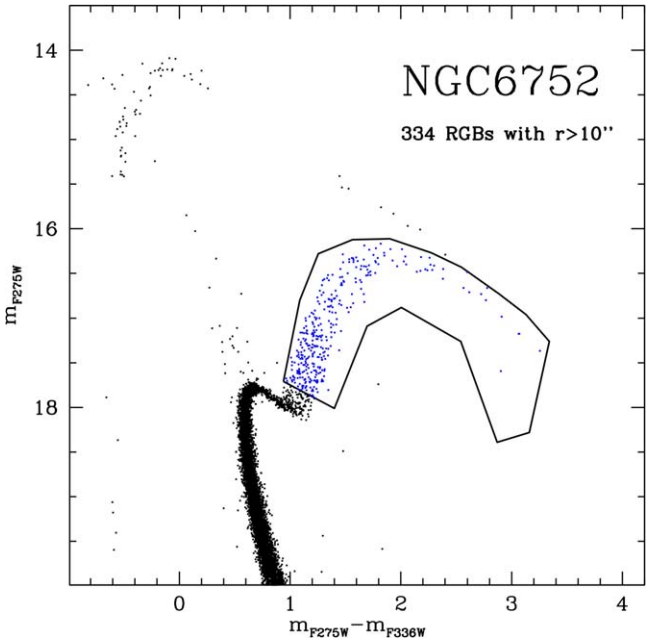

Figure 6. Selection box (black line) of the RGB sample (blue dots) in NGC 6752. The box is equal to that used in M13 (but for the color and magnitude shifts needed to align the two CMDs; see Figure 2). The number of RGB stars has been used as a normalization factor of the WD samples to account for the different intrinsic richness of the two clusters.

3.2. Comparing the WD LF of NGC 6752 and M13

For a proper comparison between the WD LFs of NGC 6752 and M13, we need to take into account the intrinsic mass of the two clusters. According to the procedure adopted in C21, we used as normalization the number of RGB stars. The stars are bright (corresponding to high completeness levels at any distance from the center), and for a given total stellar mass of the host population their number depends only on the evolutionary speed, which is the same in clusters with the same initial chemical composition and age (see, e.g., Renzini & Buzzoni 1986). Taking advantage of the excellent match obtained between the CMDs of the two clusters (see Figure 2), the RGB population was selected in the observed CMD by using the same box adopted for M13, that samples the entire RGB extension down to its base (see Figure 6). Of course, the RGB stars have been counted in the same cluster area considered for the WD selection ($r > 10''$), providing a total of 335 objects.

The completeness corrected number of WDs counted in the various magnitude bins, divided by the total number of RGB stars thus obtained, finally provided us with the WD LF normalized to the RGB reference population, shown in Figure 7 (blue circles). The corresponding normalized WD LF of M13 (from C21) is plotted in the same figure in red for comparison. Although the WD LF of NGC 6752 reaches much fainter magnitudes than that of M13, the match between the results in the two systems is really impressive, with the portions in common being almost indistinguishable. This provides strong evidence that the two clusters share the same type of WD population, suggesting that also NGC 6752 hosts a relevant fraction of slowly cooling WDs, as expected from its HB morphology.

This expectation is also consistent with the conclusion by Cassisi et al. (2014) that the mass distribution along the HB in the two clusters is essentially the same, with the large majority

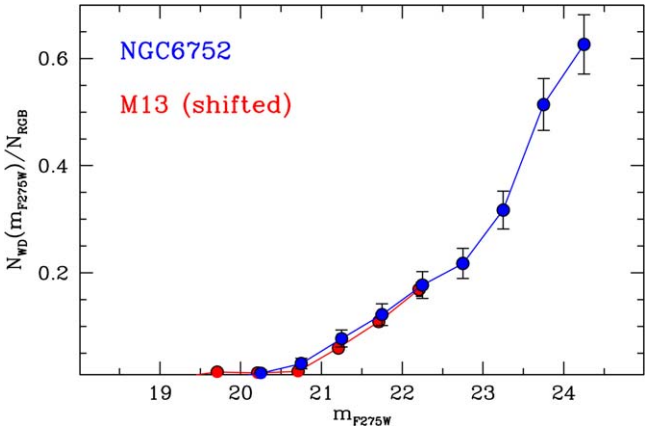

Figure 7. Completeness corrected WD differential LFs, normalized to the number of RGB reference stars, for NGC 6752 (blue circles) and M13 (red circles). The same magnitude shift adopted in Figure 2 has been applied to the LF of M13.

of HB stars having masses smaller than $\sim 0.56\,M_{\odot}$. According to theoretical models (BaSTI and Bono et al. 2020), at the considered metallicity ($Z = 0.001$), these stars do not experience the thermal pulse AGB stage during which the third dredge-up occurs. We can thus assume that, as in M13, approximately 70% of the WD progenitors in NGC 6752 end their evolution with hydrogen envelopes thick enough (a few $10^{-4}\,M_{\odot}$) to guarantee stable hydrogen burning during the subsequent WD cooling stage. The same proportion between standard and slowly cooling WDs ($\sim$30% and 70%, respectively) is therefore expected in the two clusters.

To quantitatively test this prediction, the left panel of Figure 8 compares the completeness corrected cumulative LF, normalized to the number of RGB stars, of NGC 6752 WDs (thick blue line), with the results of Monte Carlo simulations of the entire evolutionary path from the RGB, to the HB and then the WD stages, specifically computed by adopting the HB mass distributions determined for M3 and M13 (see C21). The simulation including 100% of standard WDs (as observed in M3) corresponds to the dashed line in the figure, while the run including a combination of 30% standard WDs and 70% slowly cooling WDs is marked with the black solid line. As expected, the WD LF of NGC 6752 is in impressive agreement with the latter, demonstrating that, according to the cluster HB morphology, the WD population is dominated by a relevant fraction of slowly cooling objects. For the sake of comparison, the right panel of Figure 8 shows the normalized WD cumulative LF of M13 determined by C21, together with the same models plotted in the left panel. The faintest WDs sampled in NGC 6752 have luminosities of just $\sim 10^{-2.7}\,L_{\odot}$, significantly fainter than those probed in M13. Thus the results presented in this work provide further solid support to the existence of slowly cooling WDs, and to the scenario traced in C21 about their origin.

4. Conclusions

The key points linking the presence of slowly cooling WDs in a cluster to its HB morphology can be summarized as follows.

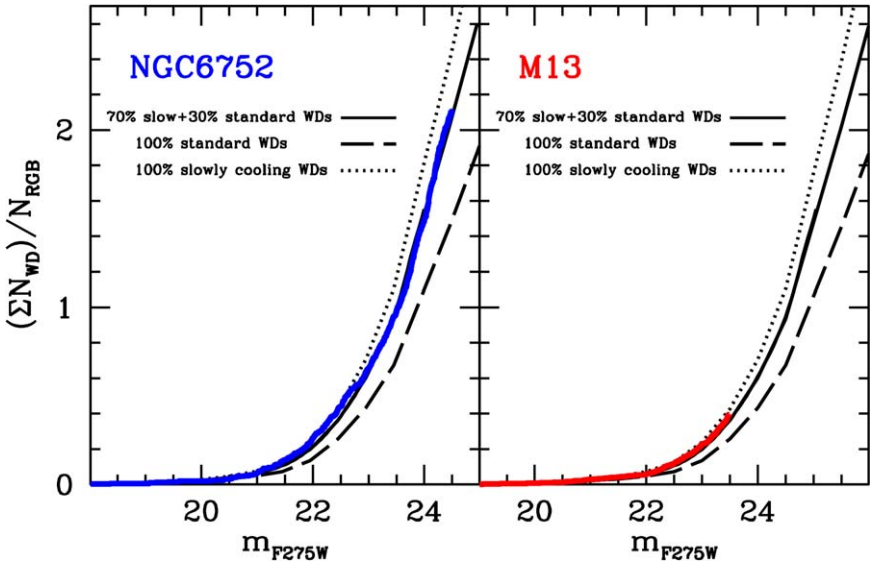

Figure 8. Left panel: WD cumulative LF of NGC 6752, corrected for completeness and normalized to the number of RGB stars (thick blue line), compared to the results of Monte Carlo simulations including 100% standard WDs (dashed line), 100% slowly cooling WDs (dotted line), and a combination of 30% standard WDs and 70% slowly cooling WDs (black solid line). Right panel: the same for M13 (red thick line, from C21).

1. The energy support responsible for slowing down the cooling process is provided by stable hydrogen burning in the WD external layers, which is made possible by the presence of a hydrogen-rich residual envelope containing enough mass (on the order of a few $10^{-4}\,M_{\odot}$; see, e.g., Renedo et al. 2010). More standard WDs like those in M3 have a hydrogen content below the threshold for hydrogen burning ignition, and thus progressively cool in time with no sources of active energy production.
2. According to Althaus et al. (2015), the third dredge-up is the crucial event regulating the mass of the residual hydrogen in proto-WDs. In fact, during the third dredge-up carbon is carried into the convective envelope and, in turn, hydrogen is brought down inside the star, where it is burned. Thus, the occurrence (or lack thereof) of the third dredge-up affects the residual hydrogen envelope of the proto-WD when it reaches its cooling track, impacting its structure and cooling time.
3. Theoretical models (e.g., Bono et al. 2020) show that at $Z = 0.001$ HB stars with masses smaller than $\sim 0.56\,M_{\odot}$ skip the thermal pulse AGB stage, where the third dredge-up occurs. This is because their envelope mass is so small that the alternate helium and hydrogen burning in shells surrounding the carbon–oxygen core cannot occur. Completely or partially skipping the AGB phase guarantees the survival of a residual hydrogen envelope in these stars when they evolve off the HB toward the WD stage; hence, they will evolve as WDs with stable hydrogen burning and a significant delay of their cooling time.
4. From stellar evolution theory it is also well known that HB stars with the above mentioned mass and metallicity populate the blue tail of the observed HBs.

As a result of this chain of events, significant populations of slowly cooling WDs are expected in globular clusters with well-populated and extended blue HB morphologies.

By showing that NGC 6752, a Galactic GC with blue extended HB morphology, hosts a large sample (∼70% of the total) of slowly cooling WDs, this work not only provides new evidence for the existence of this class of WDs, but also gives strong support to the picture above. Indeed, the fact that the same mixture of standard and slow WDs is able to reproduce the WD LFs observed in both NGC 6752 and M13, while 100% of standard WDs are needed for M3 (see C21), demonstrates the link between the cluster HB morphology and the presence of these stars, and provides empirical support to the proposed physical origin of these objects (i.e., the fact that they skip the third dredge-up). In fact, the only major difference between M3 and the other two systems is the HB morphology; at odds with M3, NGC 6752 and M13 have a (remarkably similar) blue-tail HB, which is populated by such low-mass stars that they skip the third dredge-up and evolve in slowly cooling WDs.

While the WD cooling sequence in M13 samples luminosities down to $\log(L/L_{\odot}) \sim -1.7$ (see C21), in NGC 6752 we reached luminosities 1 order of magnitude fainter, corresponding to much longer delay times with respect to the standard predictions for a pure cooling process. This is shown in Figure 9, where the cooling time delay induced by stable hydrogen burning, with respect to standard models of WDs with no burning is plotted as a function of the stellar luminosity. While the magnitude limit reached in M13 corresponds to a delay of ∼60 Myr, the limit achieved in NGC 6752 implies a delay time of ∼300 Myr, meaning that most of the faintest WDs in our adopted photometry have cooling ages of ∼760 Myr, instead of ∼460 Myr as standard models would suggest (see Figure 4).

The figure also shows that the contribution to the energy budget provided by the stable burning in the thin hydrogen-rich layer is essentially restricted to $\log(L/L_{\odot}) > -4$ for a low-mass WD ($0.54\ M_{\odot}$) at intermediate metallicity ($Z = 0.001$). According to the models, this luminosity corresponds to a cooling age of approximately 3.5 Gyr, and during this time the accumulated delay in the cooling process can be as large as 0.8 Gyr. An exhaustive exploration of the entire hydrogen burning phase down to magnitudes corresponding to at least $\log(L/L_{\odot}) \sim -4$ is thus required, to obtain an empirical

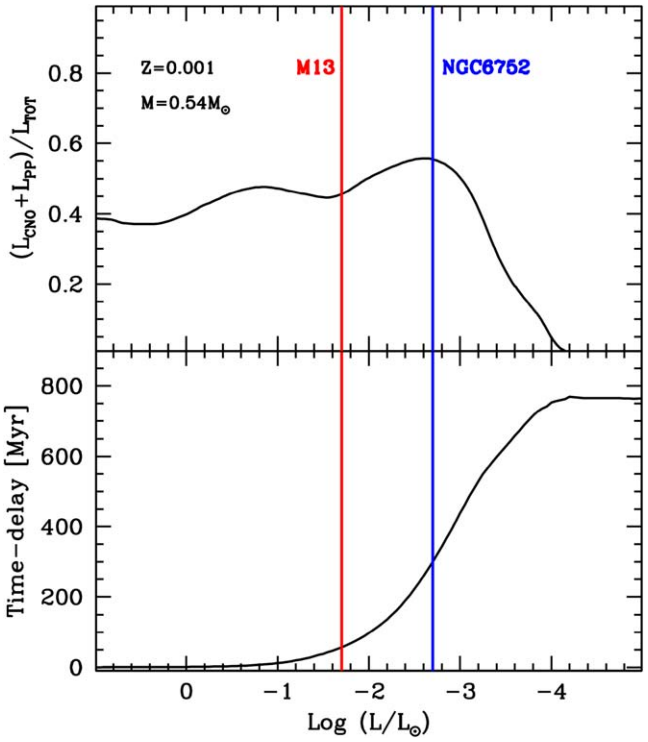

Figure 9. Top panel: contribution of stable hydrogen burning (via PP and CNO chain) to the luminosity of a low-metallicity ($Z = 0.001$), low-mass ($0.54\,M_{\odot}$) WD as a function of the luminosity. Bottom panel: delay in the cooling time induced by stable hydrogen burning, with respect to a model without burning. The two vertical lines mark the luminosity reached in NGC 6752 (present work) and in M13 (C21).

measurement of the total amount of cooling delay induced by this mechanism.

It is worth emphasizing that the predictions shown in Figure 9 refer to a single-mass WD, while the modeling of the faintest end of the WD LF is much more complex. In fact, the bright portion of the cooling sequence can be well approximated by a single-mass ($\sim 0.54\,M_{\odot}$) cooling track, but at the faintest end the contribution of WDs with larger masses must be taken into account to properly characterize the impact of the hydrogen burning on the WD LF. In the case of NGC 6752, which is the portion of the WD cooling sequence that is expected to be affected by the presence of slow WDs? As discussed above, slowly cooling WDs are the progeny of the (bluest) HB stars with a mass below $0.56\,M_{\odot}$ that skip the AGB thermal pulses. In 12–13 Gyr old clusters, the initial mass of stars on the RGB scales as $dM/dt = -0.02\,M_{\odot}\,\mathrm{Gyr}^{-1}$. Hence, given the current RGB mass in NGC 6752 ($\sim 0.8\,M_{\odot}$), we expect that about 3 Gyr ago RGB stars had a mass around $0.86\,M_{\odot}$. Under the reasonable assumption that the amount of mass lost along the RGB is approximately constant for low-mass stars of similar initial masses, this implies that about 3 Gyr ago (and even earlier in the cluster life) all the core helium burning stars had a mass above $0.56\,M_{\odot}$ and thus have all evolved through the thermal pulses along the AGB, producing "normal" WDs. Hence, all the WDs with a cooling age larger than 3 Gyr (which corresponds to $m_{\mathrm{F275W}} \sim 31$) are expected to be normal WDs, and slowly cooling WDs are predicted to affect only the portion of the WD cooling sequence brighter than $m_{\mathrm{F275W}} \sim 31$, with an importance that progressively decreases at fainter magnitudes down to this limit.

While the results presented here and in C21 provide a solid demonstration of the existence of slowly cooling WDs at intermediate metallicities ($Z = 0.001$), the extension of this investigation to fainter magnitudes and other metallicity regimes is now necessary to fully verify the theoretical predictions and provide an empirical measure of how common this phenomenon is in stellar systems. This is of paramount importance for the correct use of the WD cooling sequences as chronometers to measure cosmic ages.

This research is part of the project Cosmic-Lab at the Physics and Astronomy Department of the University of Bologna (http://www.cosmic-lab.eu/Cosmic-Lab/Home.html). The research has been funded by project *Light-on-Dark*, granted by the Italian MIUR through contract PRIN-2017K7REXT (PI: Ferraro). J.C. acknowledges the support from China Scholarship Council (CSC). M.S. acknowledges support from The Science and Technology Facilities Council Consolidated grant ST/V00087X/1.

Facilities: HST(WFC3).

Software: DAOPHOT (Stetson 1987), ALLFRAME (Stetson 1994).

ORCID iDs

Jianxing Chen https://orcid.org/0000-0002-8004-549X
Francesco R. Ferraro https://orcid.org/0000-0002-2165-8528
Mario Cadelano https://orcid.org/0000-0002-5038-3914
Maurizio Salaris https://orcid.org/0000-0002-2744-1928
Barbara Lanzoni https://orcid.org/0000-0001-5613-4938
Cristina Pallanca https://orcid.org/0000-0002-7104-2107
Leandro G. Althaus https://orcid.org/0000-0003-2771-7805
Santi Cassisi https://orcid.org/0000-0001-5870-3735
Emanuele Dalessandro https://orcid.org/0000-0003-4237-4601

References

Althaus, L. G., Camisassa, M. E., Miller Bertolami, M. M., et al. 2015, A&A, 576, A9
Annunziatella, M., Mercurio, A., Brescia, M., et al. 2013, PASP, 125, 68
Bedin, L. R., Salaris, M., King, I. R., et al. 2010, ApJL, 708, L32
Bellazzini, M., Fusi Pecci, F., Messineo, M., et al. 2002, AJ, 123, 1509
Bono, G., Braga, V. F., Fiorentino, G., et al. 2020, A&A, 644, A96
Cadelano, M., Chen, J., Pallanca, C., et al. 2020a, ApJ, 905, 63
Cadelano, M., Dalessandro, E., Webb, J. J., et al. 2020b, MNRAS, 499, 2390
Cadelano, M., Ferraro, F. R., Istrate, A. G., et al. 2019, ApJ, 875, 25
Campbell, S. W., D'Orazi, V., Yong, D., et al. 2013, Natur, 498, 198
Campbell, S. W., MacLean, B. T., D'Orazi, V., et al. 2017, A&A, 605, A98
Cassisi, S., Salaris, M., Pietrinferni, A., et al. 2014, A&A, 571, A81
Chen, J., Ferraro, F. R., Cadelano, M., et al. 2021, NatAs, 5, 1170
Cho, D.-H., Lee, S.-G., Jeon, Y.-B., et al. 2005, AJ, 129, 1922
Córsico, A. H., Althaus, L. G., Miller Bertolami, M. M., et al. 2019, A&ARv, 27, 7
Dalessandro, E., Cadelano, M., Vesperini, E., et al. 2018a, ApJ, 859, 15
Dalessandro, E., Ferraro, F. R., Massari, D., et al. 2015, ApJ, 810, 40
Dalessandro, E., Lardo, C., Cadelano, M., et al. 2018b, A&A, 618, A131
Dalessandro, E., Salaris, M., Ferraro, F. R., et al. 2013, MNRAS, 430, 459
Dotter, A., Sarajedini, A., Anderson, J., et al. 2010, ApJ, 708, 698
Ferraro, F. R., D'Amico, N., Possenti, A., et al. 2001, ApJ, 561, 337
Ferraro, F. R., Lanzoni, B., Dalessandro, E., et al. 2012, Natur, 492, 393
Ferraro, F. R., Lanzoni, B., Dalessandro, E., et al. 2019, NatAs, 3, 1149
Ferraro, F. R., Lanzoni, B., & Dalessandro, E. 2020, RLSFN, 31, 19
Ferraro, F. R., Lanzoni, B., Raso, S., et al. 2018, ApJ, 860, 36
Ferraro, F. R., Messineo, M., Fusi Pecci, F., et al. 1999, AJ, 118, 1738
Ferraro, F. R., Paltrinieri, B., Fusi Pecci, F., et al. 1997a, ApJL, 484, L145
Ferraro, F. R., Paltrinieri, B., Fusi Pecci, F., et al. 1997b, A&A, 324, 915
Ferraro, F. R., Sills, A., Rood, R. T., et al. 2003, ApJ, 588, 464

Gratton, R. G., Bragaglia, A., Carretta, E., et al. 2005, A&A, 440, 901
Gratton, R. G., Carretta, E., & Bragaglia, A. 2012, A&ARv, 20, 50
Gratton, R. G., D'Orazi, V., Bragaglia, A., et al. 2010, A&A, 522, A77
Gruyters, P., Casagrande, L., Milone, A. P., et al. 2017, A&A, 603, A37
Hansen, B. M. S., Anderson, J., Brewer, J., et al. 2007, ApJ, 671, 380
Harris, W. E. 1996, AJ, 112, 1487
Hidalgo, S. L., Pietrinferni, A., Cassisi, S., et al. 2018, ApJ, 856, 125
Jeffery, E. J., von Hippel, T., van Dyk, D. A., et al. 2016, ApJ, 828, 79
Kilic, M., Munn, J. A., Harris, H. C., et al. 2017, ApJ, 837, 162
King, I. R. 1966, AJ, 71, 64
Lanzoni, B., Dalessandro, E., Ferraro, F. R., et al. 2007, ApJL, 668, L139
Lanzoni, B., Ferraro, F. R., Alessandrini, E., et al. 2016, ApJL, 833, L29
Lanzoni, B., Ferraro, F. R., Dalessandro, E., et al. 2010, ApJ, 717, 653
Lanzoni, B., Ferraro, F. R., Dalessandro, E., et al. 2019, ApJ, 887, 176
Lapenna, E., Lardo, C., Mucciarelli, A., et al. 2016, ApJL, 826, L1
Miocchi, P., Lanzoni, B., Ferraro, F. R., et al. 2013, ApJ, 774, 151
Mucciarelli, A., Lapenna, E., Lardo, C., et al. 2019, ApJ, 870, 124
Pietrinferni, A., Cassisi, S., Salaris, M., et al. 2006, ApJ, 642, 797
Pietrinferni, A., Hidalgo, S., Cassisi, S., et al. 2021, ApJ, 908, 102
Piotto, G., Milone, A. P., Bedin, L. R., et al. 2015, AJ, 149, 91
Raso, S., Ferraro, F. R., Dalessandro, E., et al. 2017, ApJ, 839, 64
Renedo, I., Althaus, L. G., Miller Bertolami, M. M., et al. 2010, ApJ, 717, 183
Renzini, A., & Buzzoni, A. 1986, Spectral Evolution of Galaxies, Vol. 122 (Dordrecht: D. Reidel), 195
Sabbi, E., Ferraro, F. R., Sills, A., et al. 2004, ApJ, 617, 1296
Salaris, M., Cassisi, S., Pietrinferni, A., et al. 2010, ApJ, 716, 1241
Salaris, M., & Weiss, A. 2002, A&A, 388, 492
Sandquist, E. L., & Bolte, M. 2004, ApJ, 611, 323
Stetson, P. B. 1987, PASP, 99, 191
Stetson, P. B. 1994, PASP, 106, 250
VandenBerg, D. A., Brogaard, K., Leaman, R., et al. 2013, ApJ, 775, 134
Winget, D. E., & Kepler, S. O. 2008, ARA&A, 46, 157
Woosley, S. E., & Heger, A. 2015, ApJ, 810, 34